The PREHydrA: A Passive Return, High Force Density, Electro-Hydrostatic Actuator Concept for Wearable Robotics

Kyrian Staman, Allan J. Veale, and Herman van der Kooij

***Abstract*—This letter presents the Passive Return Electro-Hydrostatic Actuator (PREHydrA), an actuator for use in wearable robotics. It eliminates conventional hydraulic systems' fluid supply and valves, potentially making it lighter, more efficient, and simpler. It also avoids the configuration-dependent friction of Bowden cable transmissions. A physical port-based network model was created of the PREHydrA that predicts force tracking with a maximum error of about 4 N. Closed loop output force control was used in experiments to obtain a mean absolute tracking error below 4 N for force references from 300 N amplitude at 0.5 Hz to 20 N amplitude at 10 Hz. These forces, frequencies, and corresponding velocities (up to 0.47 m/s) demonstrate that the PREHydrA's performance is sufficient for many wearable applications.**

***Index Terms*—Hydraulic/pneumatic actuators, wearable robots, force control, calibration and identification.**

I. Introduction

DEVELOPMENT of high force density actuation technology is a constant endeavor among many fields of research, especially in wearable robotics technology for human enhancement, rehabilitation, or function restoration. Young & Ferris [1] note in their survey of lower limb exoskeletons that the majority (more than 70 % of the investigated exoskeletons) are actuated by conventional translational and rotational electromechanical actuators [2], [3]. The actuators are placed distally, or away from the trunk (often meaning at the limb or joint level) as opposed to mounted closer to the trunk (proximally). Minimizing distal mass is highly desirable for reducing the encumbrance and energy consumption of a wearable device [4].

Wearable fluid power systems in a conventional configuration (using a fluid supply and valves) have also been successfully implemented; for example, the hydraulic BLEEX [5] and SARCOS [6] exoskeletons. These devices show how human scale hydraulics can compactly actuate joints while generating high forces.

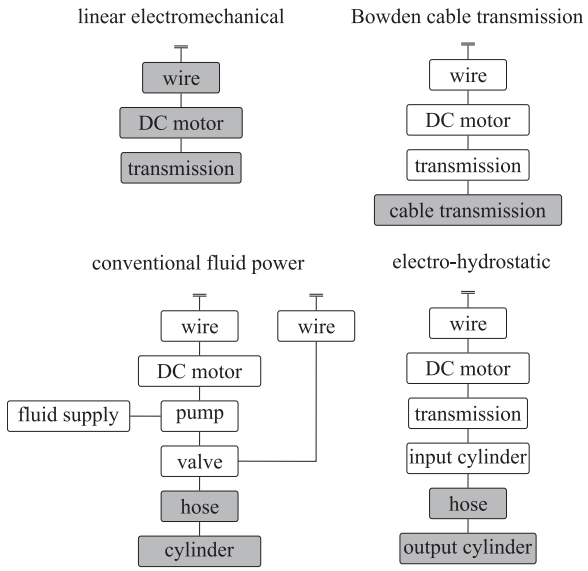

Fig. 1. Common components of various concepts for translational actuators, with distal (limb mounted) components in gray. The common components; battery, control Programmable Logic Controller (PLC), and motor drive; are omitted.

In both conventional electromechanical and fluid power actuator concepts, significant effort has to be invested to generate a wearable solution. This is shown in Fig. 1 where the left two systems represent components usually found in these types of actuators. From the electromechanical concept, it is seen that the bulk of the size and weight is carried distally. Although the hydraulic concept only places a cylinder distally, the trade-off is found in the complexity and weight of the additional required components and the inefficiencies of the pump and valve systems [5].

An alternative solution to conventional electromechanical and fluid power actuators has been presented by Veneman *et al.* [7], in which a Bowden cable transmission has been employed. This type of actuator provides a high distal force density by moving heavy components to the back of the user. The top right system of Fig. 1 shows this benefit. However, Chen *et al.* [8], have shown Bowden cable transmissions have a strongly configuration-dependent friction and can limit the force efficiency below 70%, depending on cable length and curvature.

Manuscript received February 13, 2018; accepted June 18, 2018. Date of publication July 9, 2018; date of current version August 2, 2018. This letter was recommended for publication by Associate Editor A. Ajoudani and Editor P. Rocco upon evaluation of the reviewers' comments. This work was supported by the Netherlands Organisation for Scientific Research (NWO), project no. 14429. *(Corresponding author: Kyrian Staman.)*

The authors are with the Department of Biomechanical Engineering, University of Twente, Enschede 7522 NB, The Netherlands (e-mail: k.staman@utwente.nl; a.j.veale@utwente.nl; h.vanderkooij@utwente.nl).

This letter has supplemental downloadable multimedia material available at http://ieeexplore.ieee.org, provided by the authors. The Supplementary Materials contain a video showing a simple experiment carried out using the experimental setup as described in the work. It serves to show the use of commercial components and the way in which presented experiments were carried out to track sine reference signals. This material is 37.8 MB in size.

Digital Object Identifier 10.1109/LRA.2018.2854367

Lee *et al.* [9] have even reported a torque efficiency of 62% for their gait-assisting device using Bowden cable transmissions. However, such a flexible transmission can also consist of a pneumatic or hydraulic fluid line in which the friction is not configuration-dependent, increasing the efficiency during operation and avoiding complex control strategies to compensate for friction. An example is found in the work of Buerger & Hogan [10], in which they have proposed an electro-hydrostatic actuator for use in haptic devices. Electro-hydrostatic actuation has also been used, for example, by Noël *et al.* [11], who have implemented a dual-acting (using two fluid lines) hydraulic piston in an ankle-foot orthosis and Bechet *et al.* [12], [13], who have investigated the concept for use in an elbow rehabilitation device and in a minimally invasive surgery robot.

These types of actuators are termed hydrostatic, because the fluid column acts as a single bulk mass that is driven by a positive displacement pump (also termed hydrostatic pump). These pumps convert mechanical power (velocity and force) to fluid power (flow and pressure) by non-slipping, ideally leak-free operation, using a closed fluid system. They are characterized by low bulk fluid velocities and instantaneous buildup of pressure. The removal of conventional systems' fluid supply and valves potentially makes hydrostatic systems lighter, more efficient, and simpler. The electro-hydrostatic actuator concept is shown in the bottom right of Fig. 1. It has neither the configuration-dependent friction of Bowden cables nor the inefficiency of hydraulic valves. However, the disadvantage is that hydrostatic actuators require all components for every actuator, whereas conventional hydraulics can actuate multiple outputs using a single pump and valve.

Although this electro-hydrostatic concept has some advantages and has been proposed previously, it has not been investigated as extensively as electromechanical actuators have been for use in wearable devices. This is due to the lack of commercially available hydraulic components for small-scale systems, which in this context means human muscle scale, with sizes, weights, and powers of the order of 100 mm, 200 g, and 100 W, respectively. Since designing and manufacturing components is time-consuming, most researchers have resorted to the use of miniature off-the-shelf pneumatic components in hydraulic systems. However, the limited operating pressures of pneumatic components limit their force density compared to what could be achieved if they were designed to operate at hydraulic pressures [14].

This letter presents the PREHydrA (Passive Return Electro-Hydrostatic Actuator), an electro-hydrostatic actuator using cylinders in a single-acting configuration with a return force element. The aim is to increase the force range of previous work [10] from 70 N to 400 N, while operating at velocities up to 0.4 m/s. A control strategy to compensate cylinder friction is proposed and experimental force tracking performance investigated to obtain an actuator suitable for wearable robotics. An analysis of the concept, using commercial components, is given in Section II, followed by a description of the model in Section III. The experimental setup and obtained measurement results are described in Section IV. Section V discusses the presented findings. The main conclusion is presented in Section VI.

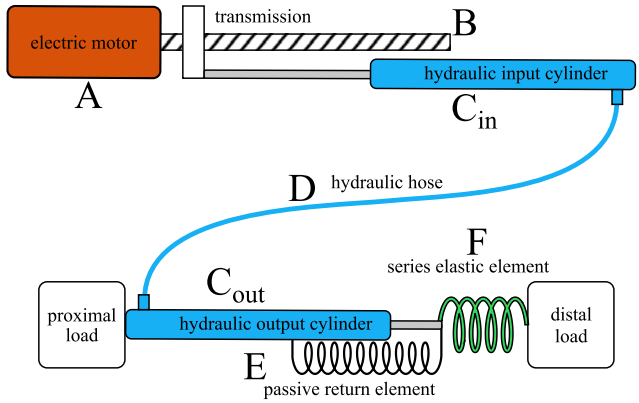

Fig. 2. Schematic of the PREHydrA concept, with electric motor (A), linear transmission (B), and input cylinder (C_{in}). The flexible hydraulic transmission (D), output cylinder (C_{out}), passive return element (E), and series elastic element (F) are placed between a proximal and distal body segment spanning a joint.

II. Concept Analysis

In this section, a qualitative analysis of key components of the PREHydrA concept is given. A schematic overview of the involved components, as shown in Fig. 1, is shown in Fig. 2. The battery, control PLC, and motor drive are omitted, because the selection of these components follows from the requirements of a specific application. Assuming the electric motor provides rotational motion, a transmission is required to provide the translational motion that drives the input cylinder. In both Fig. 2 and the experimental setup described in Section IV, this is a ball screw. Used for its high efficiency, this component could be any linear transmission and ideally should have high efficiency, low hysteresis, low volume, low mass, and could be integrated with the electric motor and input cylinder. A hose is required to act as a conduit for the fluid to deliver power to the output cylinder. Part of the hose and the output cylinder are the distal components of the actuator, while the input cylinder and everything before it can be worn on the user's back or can be grounded, creating a tethered device. This is the principle of remote actuation, where heavy components are placed away from the end-effector to reduce end-effector inertia.

Further, the PREHydrA concept uses only a single fluid line, creating a single-acting system. The advantage is that half the length of hosing is required and half the amount of hydraulic fluid with respect to dual-acting systems. This reduces mass, but also minimizes the effect of parasitic stiffness of the hoses on the limb segments. Another significant advantage of the single-acting configuration is that only one piston seal is required per cylinder, eliminating the need for a rod seal and its associated friction [15]. Also, a single fluid column allows for easier filling procedures.

The drawback of a single-acting configuration is that only unidirectional work (pushing) can be delivered, much like a Bowden cable transmission can only pull. If bidirectional force and motion are required, an element must be added that provides these. A passive solution is storing energy in a spring element that facilitates the return motion. The PREHydrA return spring

element could be designed to provide any return force profile, depending on the application.

The PREHydrA may also use a series elastic element to connect the output cylinder to the distal load. Series elastic elements are often used in human wearable actuation [1] due to the advantages of improving backdrivability, high fidelity force control, and increased energy efficiency [16]. The disadvantage is the mass and volume of the additional components. Hence, the suitability and design of the PREHydrA's series elastic element must be determined based on the application, for example by analyzing the interaction stiffness of the device the PREHydrA is used in.

III. Actuator Model

In this section, a model is presented that was developed of the PREHydrA concept based on commercially available components as listed in Section IV, Table II. The hydraulic cylinders are, with an inner diameter of 14.3 mm, among the smallest bore cylinders that were available off-the-shelf. The output cylinder was modeled in a configuration in which the proximal and distal loads of Fig. 2 are fixed, since the loads are application-specific and the hydrostatic components were of primary interest. This caused the series elastic and the passive return elements to become parallel, simplifying the analysis. Therefore, in the remainder of this work, the series elastic element is omitted. The passive return element was assumed to provide a force linearly proportional to piston displacement. This model was used to investigate critical concept components and will eventually help to design small-scale hydraulic cylinders to develop an electro-hydrostatic actuator for use in wearable robotics.

The concept actuator as presented was modeled using a port-based network description of physical systems (using SimScape within the Simulink environment of Matlab). The model includes motor drive control parameters, motor dynamics, ball screw efficiency, masses of cylinder pistons, rods and other components, fluid characteristics, and cylinder friction (as explained below). Further, cylinder connection ports and hose fittings were modeled as orifices. Halfway along the hose, the pressure sensor block in the experimental setup was also modeled by orifices. The hose model incorporates friction loss across its length, based on the flow regime and compressibility of the fluid.

Seal leakage is neglected as it was expected not to influence short-term actuator performance significantly. Since refilling of the experimental setup was not required during experiments, this assumption seems reasonable. Fluid inertia was also neglected, because accelerations were expected to be low. For the experimental setup, a volume of about 56 mL of hydraulic fluid was required. Using a water-glycol solution as listed in Section IV, Table II, the fluid mass is 60 g, which is 8% of the total moving mass in the setup.

A. Friction Identification

Although accurate models of friction have been proposed [17], specifically for hydraulic cylinders, the identified model for this concept analysis was a straightforward, yet sufficient, adaptation of a model that includes Coulomb and viscous friction and the Stribeck effect [18]. The Coulomb component assumes a certain preload between the O-ring seals and the cylinder wall and a linear increase in the static friction based on the pressure that squeezes the seals against the cylinder wall. This simplified approach was chosen to investigate the effect of cylinder friction on the performance of the PREHydrA. The friction model is given by:

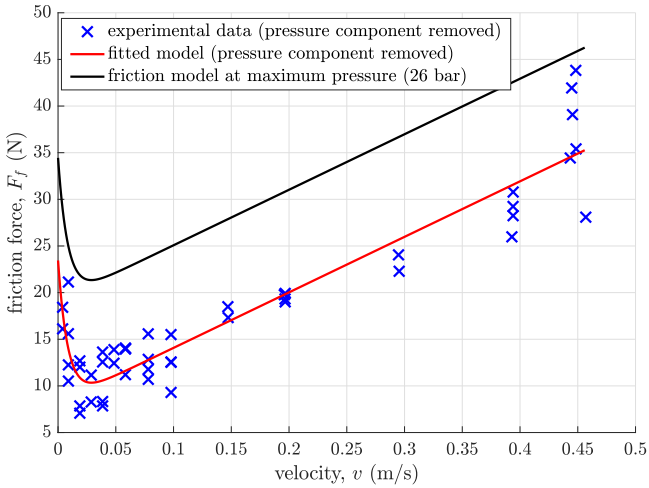

Fig. 3. Identified friction characteristic for one cylinder.

$$F_f = (F_C + F_{S,0}e^{-c|v|})\text{sign}(v) + f_v v \tag{1}$$

$$F_C = F_{preload} + f_C p \tag{2}$$

Where F_f is the friction force, F_C the Coulomb friction, $F_{S,0}$ the maximum Stribeck force, and $F_{preload}$ the pressure independent part of the Coulomb friction, all in N. The constant c is the Stribeck exponential rate of decay in s/m, f_v is the viscous friction coefficient in Ns/m, and f_C is the Coulomb friction pressure coefficient in N/Pa. The friction force is a function of velocity v in m/s and the pressure p, in Pa. The discontinuity at zero velocity was implemented numerically as a linear relation between -1×10^{-4} and 1×10^{-4} m/s to avoid computational difficulties.

An experimental friction identification was carried out by driving the input cylinder at a constant velocity. The difference between measured input and output force was assumed to be due to friction. This means that the fluid friction, spring damping, and other minor dissipating effects are subsumed in this measurement. Evaluation of the model supported the assumption that these effects were negligible. Identification was carried out up to a velocity of 0.45 m/s, limited by the performance of the electric motor, but sufficient for wearable actuator technology. The identified friction model is shown in Fig. 3, in which the pressure component ($f_C p$) has been removed. This is done by calculating f_C using the increasing force difference and pressure. Now a friction model is obtained without pressure dependence. The pressure dependence is significant, seeing that the maximum encountered pressure of 26 bar (at 300 N amplitude experiments) adds about 10 N to the friction force, as also indicated in Fig. 3. The model parameters are listed in Table I.

TABLE I
IDENTIFIED FRICTION PARAMETERS FROM EQUATIONS (1), (2)

Parameter	*Identified value*	*Standard error*
$F_{preload}$	$8.1\ (N)$	$0.91(N)$
f_C	$4.2 \times 10^{-6}\ (N/Pa)$	N.A.
$F_{S,0}$	$15.3\ (N)$	$5.96(N/Pa)$
c	$118.5\ (s/m)$	$61.1(s/m)$
f_v	$59.5\ (Ns/m)$	$3.56(Ns/m)$

TABLE II
EXPERIMENTAL SETUP COMMERCIAL COMPONENTS

#	*Component*
1	Kollmorgen S20260-VTS, 240 V AC, brushless servo drive
2	Kollmorgen AKM22C-BCNC-00, 0.84 Nm, 290 W servomotor
3	Ruland PCMR25-8-8-A aluminium flexible coupling
4	SKF 7200 BEP angular contact ball bearing
5	Misumi BSSR1405-325-RLC, 5 mm lead, rolled ball screw
6	ATI mini45-E six-axis force/torque transducer
7	Clippard H9C-6D brass cylinders (modified)
8	Eurol Coolant XL -36, 50% ethane-1,2-diol coolant
9	generic M6 car brake bleed screw
10	Parker GE08LR1/8EDOMD, male stud connector
11	Parker 550H, 0.5 m thermoplastic hydraulic hose
12	Measurement Specialties EPX-N02-150B-Z2 pressure sensor
13	Amatec E1000-115-7000M, 1420 N/m extension spring
14	ATI 9105-IFPS-1 DAQ interface power supply
15	National Instruments 6225 M-series DAQ PCI card

The cylinder friction is nonlinear and significant with a range from 7 to 44 N over the tested velocities. Without a suitable controller, such friction will reduce the ability of the PREHydrA to reproduce a desired motion or force reference.

B. Output Force Control

The main performance metric of the presented actuator concept will be the accuracy with which representative forces can be tracked in the presence of friction and unmodeled (or inaccurately modeled) system characteristics. The overall question is whether this performance is sufficient for use in wearable technology. The output force of the PREHydrA, as shown in Fig. 2, is the force it produces between the proximal and distal segments. With these segments fixed, the output motion is against the passive return element, as described in Section III.

To compensate for cylinder friction, the motor drive used an internal feedback controller to control the velocity of the motor and input cylinder piston. The desired velocity control signal is obtained from a forward fed reference force. This force is linearly proportional to the output cylinder velocity as estimated by means of the passive return spring stiffness. This is shown in the block diagram in Fig. 4 by the relation given below:

$$v_{FF} = \frac{\mathrm{d}}{\mathrm{d}t}\frac{F_{ref}}{k} = \dot{x}_{ref} \tag{3}$$

Where v_{FF} is the feedforward velocity signal in m/s, F_{ref} is the reference force in N/s, k is the spring stiffness in N/m, and x_{ref} is the reference position in m.

A feedback loop is closed on the measured output force, F_{out} in N, to compensate for the drift arising from velocity tracking errors, non-linear (and unidentified) spring behavior, and other remaining errors and disturbances. A proportional feedback controller is used with a gain, k_p, of 0.001 m/Ns, acting on the force error, e_F. This is also shown in Fig. 4.

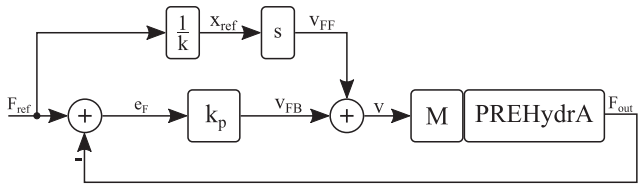

Fig. 4. Block diagram of the output force control strategy, excluding motor velocity control. M denotes the motor drive controllers and hardware, connected to the PREHydrA.

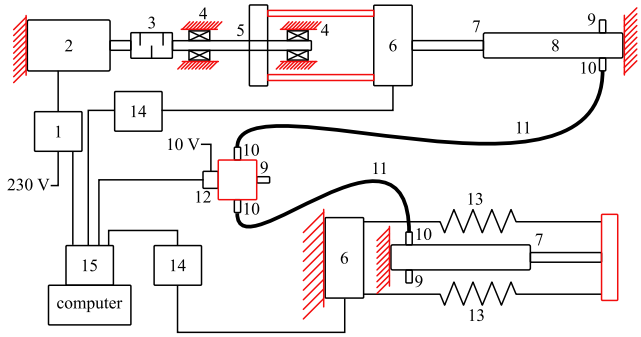

Fig. 5. Schematic representation of test setup components; commercial components are numbered and listed in Table II; components in red are custom aluminium parts.

IV. EXPERIMENTAL RESULTS

To identify cylinder friction and validate the model, an experimental setup was developed in which the proximal and distal loads were fixed, as discussed in Section III. A schematic representation of the experimental setup is shown in Fig. 5, with the components listed in Table II. All components used in the setup are commercially available, except for the custom aluminium mounting components and base plate. With the cylinders mounted horizontally, the effect of gravity on the actuation was minimized.

Careful filling and air bleeding of the system was important to ensure the incompressibility of the PREHydrA's fluid column. This process was facilitated by the setup's design. The highest point in the setup was the connector block located halfway along the fluid hose. A bleed screw was integrated in this connector block to allow for air bleeding both during and after filling. Two identical bleed screws were integrated into the commercial cylinders and were used as filling points. Filling the system from the cylinder chambers up into the hose and out of the top bleed screw ensured that a minimal amount of air was trapped in the system. After initial filling, the setup was moved back and forth to allow any remaining air to make its way up to the bleed screw; the air was bled from the system and a small amount of hydraulic fluid was inserted by syringe to fully fill the system. This second procedure was repeated as maintenance at the start of a set of experiments.

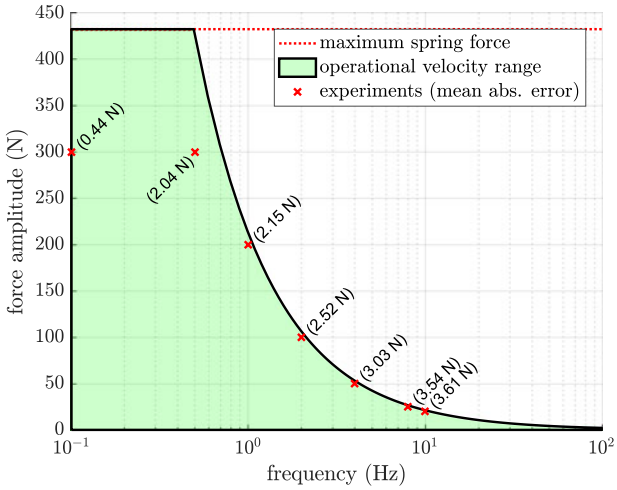

Fig. 6. Operational range of sinusoidal reference force amplitudes as a function of reference frequency, as based on actuator limits. Markers show experimentally obtained force tracking error for selected reference frequencies.

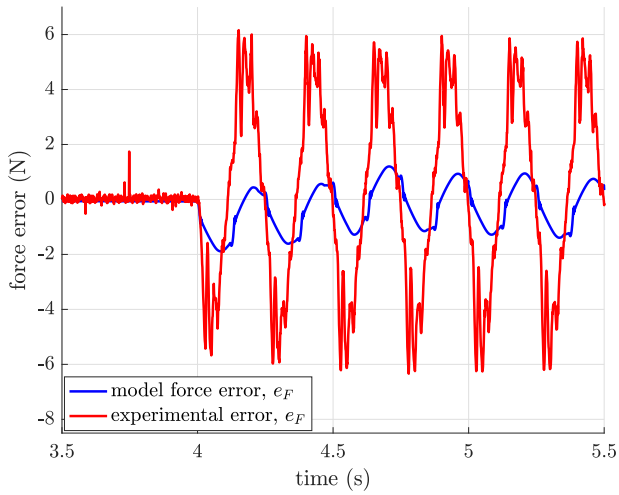

Fig. 7. Tracking force errors of model and measurement for reference of 50 N amplitude and 4 Hz frequency.

As shown in Fig. 5, the two springs were implemented as extension springs to prevent difficulties with buckling. They were attached to the carriage and load cell by Dyneema string to minimize strain. The data acquisition computer shown in Fig. 5 was a dedicated Simulink Real-Time target computer on which the control models generated from Simulink were executed.

Given the stiffness of the return springs and cylinder stroke, the maximum force that can be tested in this setup was 433 N. This is representative of the forces required for wearable linear actuators for use in assistive devices. The maximum translational velocity is dictated by the motor's maximum mechanical speed of 592 rad/s, corresponding to a maximum input cylinder velocity of 0.47 m/s. Given a sinusoidal force reference, this maximum velocity constrained the reference's amplitude as a function of its frequency. The feedforward path from Fig. 4 gives the relation between reference force and motor velocity as a function of reference frequency:

$$F_{ref} f_{ref} = \left| \frac{\omega_{\max} k i}{j 2\pi} \right| = 213 \ (N/s) \tag{4}$$

Where F_{ref} is the reference force amplitude in N and f_{ref} the reference sine frequency in Hz. The maximum motor speed, $\omega_{\max} = 592$ rad/s, the spring stiffness $k = 2840$ N/m, and the ball screw transmission ratio $i = 5 \times 10^{-3}/2\pi$ m/rad. The force-frequency operational range of the actuator is shown in Fig. 6. The force reference signals included a 45 N offset to compensate for the pretension of the return springs and a 50 N margin with respect to the maximum force, keeping the PREHydrA's cylinders away from their end stops. This offset is applied using a skewed sine step equal to the offset plus the amplitude over 2 seconds, after which the harmonic signal (a cosine) starts. The reference signal is thus ensured to be continuous and smooth, which is required for the feedforward derivative. The maximum tested force amplitude was 300 N.

Fig. 7 shows the tracking error of the 50 N, 4 Hz sine reference experiment and model prediction. A maximum error of 6.44 N is observed with a mean absolute error of 3.03 N over the sine part of the signal. The model from Section III predicted a maximum tracking error of about 4 N less. As shown in Fig. 7, the highest tracking error occurred at the extrema of the reference. This is where the direction of motion of the actuator reversed and the influence of the cylinder seal static friction reduced tracking accuracy. Note that the error is the difference between the reference signal and the model predicted or measured output cylinder force. The mean absolute error is the arithmetic mean of the absolute of these errors.

Similar tracking results were obtained for force references with frequencies ranging from 0.1 to 10 Hz and corresponding amplitudes ranging from 300 to 20 N. As shown in Fig. 6, the mean absolute errors were of a similar order of magnitude across the experiments, except for the lowest frequency experiment, varying from 0.44 to 3.61 N. The general behavior of the error across experiments was also similar. This indicates that there is a portion of the cylinder friction (stick slip) of about 6 N (see Fig. 7) that is not compensated by the controller. Further, nonlinearity of the return spring and other unmodeled characteristics of the system reduced tracking accuracy.

To clarify the concept actuator setup as shown in Fig. 5, a video of a sine tracking experiment on the experimental setup is available at http://ieeexplore.ieee.org.

V. Discussion

The concept was analyzed and from results of friction identification experiments it was concluded that the magnitude and nonlinearity of cylinder friction were the main cause of inaccuracy in the PREHydrA's reference tracking. An intuitive control method to compensate friction and control the output force was presented. Finally, error tracking results from both the model and an experimental setup were compared for a range of forces and velocities representative of wearable applications.

In wearable applications, such as exoskeletons and powered orthoses, wearability entails minimum device size and mass. As such, the current choice of separate ball screw, electric motor,

and input cylinder reduced wearability of the system. A more compact and lightweight design would integrate these components. The distal mass is roughly 500 g, for the cylinder and springs. Operating at the maximum rated pressure of the cylinders of 70 bar, the delivered force will be about 1000 N, resulting in a force density of 2000 N/kg. This is equivalent to pneumatic components, but is low for hydraulic systems. The high mass of small scale commercial cylinders with respect to their expected mass [14], degenerates the force density. Also, the force density of the current experimental setup could be significantly higher if it was operated at higher pressures. A maximum observed pressure during experiments of 26 bar (for the 300 N amplitude experiments) is low with respect to the rated operating pressure of hydraulic components. Smaller cylinders for use with higher pressures, although optimal for use in the PREHydrA, are commercially not available.

As shown, the main factor that reduces the force efficiency is the cylinder friction. The maximum friction (about 45 N) is observed at maximum velocity and pressure. This maximum pressure occurs when maximum force (300 N) is delivered, resulting is a force efficiency of 87 percent. This is comparable to other actuator concepts and an improvement over Bowden cables.

A further design consideration is that of the passive return element, which in this work was a linear spring. This provided a linearly increasing return force with displacement, that was sufficient for the experiments presented in this work. Other return elements are possible, such as the constant force element used by Buerger & Hogan [10], or hyperelastic (natural rubber) cord used by Masood *et al.* [19] in a rotary exoskeleton joint. This shows a given application requires its own return force behavior. Hence, the passive return element should be designed based on the specific application of the PREHydrA, taking into account requirements on, for example, force profile, mass, volume and robustness.

The friction identification experiments were conducted to obtain a model and investigate the effects of friction on performance. Although the identification of the nonlinear friction behavior for low velocities was uncertain, model predictions are still accurate to within 4 N. Further, two assumptions were done; the friction behavior is symmetric with respect to direction of motion and it is independent of current piston location within the stroke. Both these assumptions need to be carefully considered when performing experiments on commercial hydraulic cylinders, because the manufacturing process and assembly can introduce direction and location-dependent characteristics.

Future work will be directed towards developing the PREHydrA concept for application in exoskeleton technology for gait restoration and improving the force density and compactness to obtain a high performance wearable actuator.

VI. Conclusion

This work presented the PREHydrA, a passive return electrohydrostatic actuator with a four times larger output force range with respect to previous work, with no loss in velocity or tracking performance. Forces between 300 N at 0.5 Hz and 20 N at 10 Hz were tracked with a mean absolute error below 3.7 N.

Using the developed model and performed experiments, it is shown that system parameters can be obtained and force tracking performance can be sufficiently realized using a straightforward control strategy, resulting in an actuator concept suitable for application in wearable robotics.

References

[1] A. J. Young and D. P. Ferris, "State of the art and future directions for lower limb robotic exoskeletons," *IEEE Trans. Neural Syst. Rehabil. Eng.*, vol. 25, no. 2, pp. 171–182, Feb. 2017.

[2] J. Pratt, B. Krupp, C. Morse, and S. Collins, "The RoboKnee: An exoskeleton for enhancing strength and endurance during walking," in *Proc. IEEE Int. Conf. Robot. Automat.*, Apr. 2004, vol. 3, pp. 2430–2435.

[3] A. Esquenazi, M. Talaty, A. Packel, and M. Saulino, "The ReWalk powered exoskeleton to restore ambulatory function to individuals with thoracic-level motor-complete spinal cord injury," *Amer. J. Phys. Med. Rehabil.*, vol. 91, no. 11, pp. 911–921, Nov. 2012.

[4] R. Browning, J. Modica, R. Kram, and A. Goswami, "The effects of adding mass to the legs on the energetics and biomechanics of walking," *Med. Sci. Sports Exercise*, vol. 39, no. 3, pp. 515–525, Mar. 2007.

[5] A. Zoss and H. Kazerooni, "Architecture and hydraulics of a lower extremity exoskeleton," in *Proc. ASME Int. Mech. Eng. Congr. Expo.*, Nov. 2005, pp. 1447–1455.

[6] S. Karlin, "Raiding Iron Man's closet [Geek Life]," *IEEE Spectr.*, vol. 48, no. 8, p. 25, Aug. 2011.

[7] J. Veneman, R. Ekkelenkamp, R. Kruidhof, F. van der Helm, and H. van der Kooij, "Design of a series elastic- and Bowden cable-based actuation system for use as torque-actuator in exoskeleton-type training," in *Proc. 9th Int. Conf. Rehabil. Robot.*, Jun. 2005, pp. 496–499.

[8] D. Chen, Y. Yun, and A. D. Deshpande, "Experimental characterization of Bowden cable friction," in *Proc. IEEE Int. Conf. Robot. Automat.*, May 2014, pp. 5927–5933.

[9] Y. Lee *et al.*, "Biomechanical design of a novel flexible exoskeleton for lower extremities," *IEEE Trans. Mechatronics*, vol. 22, no. 5, pp. 2058–2069, Jun. 2017.

[10] S. P. Buerger and N. Hogan, "Novel actuation methods for high force haptics," in *Advances in Haptics*, M. H. Zadeh, Ed. London, U.K.: InTech, Apr. 2010.

[11] M. Noël, B. Cantin, S. Lambert, C. M. Gosselin, and L. J. Bouyer, "An electrohydraulic actuated ankle foot orthosis to generate force fields and to test proprioceptive reflexes during human walking," *IEEE Trans. Neural Syst. Rehabil. Eng.*, vol. 16, no. 4, pp. 390–399, Jun. 2008.

[12] F. Bechet and K. Ohnishi, "Electro-hydraulic force transmission for rehabilitation exoskeleton robot," in *Proc. IEEE 13th Int. Workshop Adv. Motion Control*, 2014, pp. 260–265.

[13] F. Bechet, K. Ogawa, E. Sariyildiz, and K. Ohnishi, "Electrohydraulic transmission system for minimally invasive robotics," *IEEE Trans. Ind. Electron.*, vol. 62, no. 12, pp. 7643–7654, Jul. 2015.

[14] J. Xia and W. K. Durfee, "Analysis of small-scale hydraulic actuation systems," *J. Mech. Des.*, vol. 135, no. 9, pp. 1–11, Jul. 2013.

[15] A. Campos and W. K. Durfee, "Experimental validation of an analytical model for O-ring friction and leakage at high pressure," Univ. Minnesota Digital Conservancy, Minneapolis, MN, USA, Tech. Rep., 2015.

[16] J. Pratt, B. Krupp, and C. Morse, "Series elastic actuators for high fidelity force control," *Ind. Robot: Int. J. Robot. Res. Appl.*, vol. 29, no. 3, pp. 234–241, 2002.

[17] X. Tran, W. Khaing, H. Endo, and H. Yanada, "Effect of friction model on simulation of hydraulic actuator," *Proc. Institution Mech. Engineers, Part I, J. Syst. Control Eng.*, vol. 228, no. 9, pp. 690–698, Jun. 2014.

[18] H. Olsson, K. Åström, C. Canudas de Wit, M. Gäfvert, and P. Lischinsky, "Friction models and friction compensation," *Eur. J. Control*, vol. 4, no. 3, pp. 176–195, 1998.

[19] J. Masood, J. Ortiz, J. Fernández, L. Mateos, and D. Caldwell, "Mechanical design and analysis of light weight hip joint parallel elastic actuator for industrial exoskeleton," in *Proc. 6th IEEE Int. Conf. Biomed. Robot. Biomechatronics*, 2016, pp. 631–636.